

Research Article

Synthesis, Structural and Spectroscopic Portrayals of Tow Novel Biological and Photoluminescent Materials Based on Lindqvist and Keggin Heteropolyoxotungstates

Ahlem Maalaoui¹, Olivier Pérez² and Samah Toumi Akriche^{1*}

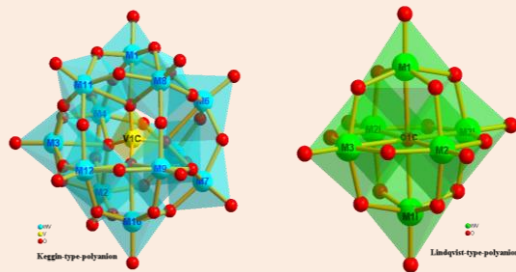
¹ Laboratoire de Chimie des Matériaux, Faculté des Sciences 7021 Zarzouna, Bizerte, Tunisie

² Laboratoire de Cristallographie et Sciences des Matériaux (CRISMAT), UMR CNRS 6508, Ensicaen, France

Abstract

Tow novel V-substituted polyoxotungstates based on V-substituted Lindqvist-type $[V_2W_4O_{19}]^4-$ and Keggin-type $[V(V_3W_9)O_{40}]^{6-}$ heteropolyoxotungstates, decorated respectively with ethylenediammonium (enH_2) and imidazolinium (ImH) cations; $(enH_2)_2[V_2W_4O_{19}].2H_2O$ ($EnV2W4$) and $(ImH)_6[V(V_3W_9)O_{40}]$ ($ImV4W9$). They are synthesized and characterized by powder and single-crystal XRD methods, ICP and elemental analysis, IR, UV-Vis and photoluminescence spectroscopy measurements and thermogravimetric analysis. X-Ray diffraction studies reveal that $EnV2W4$ crystallizes in the monoclinic space group $P2_1/c$ with $a = 8.9425 (6)$ Å, $b = 8.4976 (6)$ Å, $c = 15.2116 (11)$ Å and $\beta = 90.640 (3)^\circ$, and $ImV4W9$ crystallizes in the triclinic system with space group $P\bar{1}$ with $a = 10.297 (5)$ Å, $b = 12.015 (5)$ Å, $c = 21.231 (5)$ Å, $\alpha = 83.205 (5)^\circ$, $\beta = 83.788 (5)^\circ$ and $\gamma = 82.980 (5)^\circ$ and their crystal packing displays 3D-supramolecular assemblies of encapsulated inorganic anionic frameworks by means organic cations through electrostatic and a set of hydrogen bond interactions. Furthermore, the electronic properties and the optical band gaps are also investigated, well confirming the semiconductor behavior and

photoluminescent possessions of reported materials. In addition, the biological activities of the tow asynthesized compounds against six pathogenic microbes are also tested showing promising antimicrobial activities.



Keywords: Polyoxotungstates, X-Ray diffraction, photoluminescence, optical band gaps, antimicrobial activity

*Correspondence

Prof. S. T. Akriche,
Email: toumiakrliche@yahoo.fr

Introduction

Heteropolyoxometalates (HPOMs) are the most explored subset of polyoxometalates (POMs) including heteroanion template. It represents a great class of mixed addenda cluster anions which are fascinated in many fields such as catalysis, photochemistry, magnetic properties and medicinal and materials sciences [1-4] owing to other special possessions, like the low reduction potentials, suitable size and compositional variety [4-6], as well as structural versatility. Most of the structures in this class of compounds belong from several well known polyoxidoanions, such as Keggin, Lindquist and Dawson anion, or their substituted derivatives, which are the basis for numerous POMs.

A large number of V(V)-substituted Keggin-and Lindqvist type structures are considered as good catalysts, antimicrobial and antiviral agents because of the additional properties made by the heteroanion substituent, as evidenced in earlier reported materials such as V(V)-substituted heteropolyoxotungstates acting as insulin mimetic agents [7] and heteropolyoxotungstoantimonate as an effective antiviral agent against severe viruses [8, 9].

Currently, some V(V)-substituted keggin are well defined, for example $[\text{Ni}(\text{phen})_3]_2[\text{PVW}_{11}\text{O}_{40}]\cdot 4\text{H}_2\text{O}$ [10], $[\text{Co}(\text{phen})_3]_2[\text{PVW}_{11}\text{O}_{40}]\cdot 2\text{H}_2\text{O}$ [11], $(\text{n-Bu}_4\text{N})_3[\text{SVW}_{11}\text{O}_{40}]\cdot 0.5\text{H}_2\text{O}$ [12], $(\text{TBA})_4[\text{XV}_2\text{W}_{10}\text{O}_{38}(\mu-\text{OH})_2]$ and $(\text{TBA})_4[\text{XV}_2\text{W}_{10}\text{O}_{38}(\mu-\text{O})]$ ($\text{X} = \text{Ge, Si}$) [13], $[\text{Cu}(\text{phen})_2]_2[\text{PVW}_{11}\text{O}_{40}]$ [14], $\text{K}_3[\text{PV}_3\text{W}_9\text{O}_{40}]\cdot 19\text{H}_2\text{O}$ [15]. However, those of formula $[\text{V}(\text{V}_x\text{W}_{12-x})\text{O}_{40}]^{(3+x)^-}$ ($x = 1, 2, 3$), where the central tetrahedron is exclusively occupied by V^{V} and the remaining metal atom sites are statistically occupied by V^{V} and W^{VI} [16], are less investigated. Up to now few compounds are cited $(\text{n-Bu}_4\text{N})_4[\text{V}(\text{VW}_{11})\text{O}_{40}]$ [17] and $(\text{C}_3\text{H}_{12}\text{N}_2)_3[\text{V}(\text{V}_3\text{W}_9)\text{O}_{40}]\cdot \text{H}_2\text{O}$ [18]. For V(V)-substituted Lindqvist some examples are reported; $[\text{Cu}(\text{phen})(\text{H}_2\text{O})_3]_2[\text{V}_2\text{W}_4\text{O}_{19}]$ [7], $[\text{Cu}(\text{bpy})(\text{H}_2\text{O})_2][\text{V}_2\text{W}_4\text{O}_{19}]\cdot 4\text{H}_2\text{O}$ [19], $[\text{Ni}(\text{bpy})_3]_2[\text{V}_2\text{W}_4\text{O}_{19}]$ [20], $\text{Co}(\text{H}_2\text{O})_6\text{K}_2\text{V}_2\text{W}_4\text{O}_{19}$ [21], $[\text{Co}(\text{H}_2\text{O})_6]_2\text{V}_2\text{W}_4\text{O}_{19}$ [21], $(\text{C}(\text{NH}_2)_3)_5\text{H}(\text{V}_2\text{W}_4\text{O}_{19})\cdot \text{H}_2\text{O}$ [22].

In light of this reason, we explore a novel di-V-substituted Lindqvist-type polyoxotungstate decorated with ethylenediammonium cations and a new-fangled tri-V-substituted Keggin-type polyoxotungstate associated to a pyrrole groups with two potential N-donor sites, the imidazolinium cations. We debate herein, their structural and spectroscopic properties as well as their antimicrobial activities.

Experimental

Materials and Reagents

All reagents were purchased commercially and used without further purification.

Elemental analyses (C, H, and N) were performed on a Perkin-Elmer 2400 CHN elemental analyzer. V and W were analyzed on ICP-AES Inductively Coupled Plasma spectrometer.

The IR spectra were obtained on a Perkin-Elmer Spectrum BXII spectrometer using a sample dispersed in a spectroscopically pure KBr pellet in the $400\text{--}4000\text{ cm}^{-1}$ region.

UV—Vis spectra were recorded on a Perkin Elmer Lambda 19 spectrophotometer in the $200\text{--}800\text{ nm}$ range of the hexametalate.

Emission spectra were obtained on a Perkin-Elmer LS55 spectrofluorometer equipped with a 450 W xenon lamp as the excitation source using solid samples at room temperature.

Synthesis of EnV2W4

A mixture of $\text{Na}_2\text{WO}_4\cdot 2\text{H}_2\text{O}$ (1.32 g, 4 mmol) and V_2O_5 (0.18 g, 1 mmol) was dissolved in distilled water (30 mL) with stirring at $50\text{ }^\circ\text{C}$ for about 20 min and the pH of the solution was adjusted to 1.8 with a 4M HCl solution. Afterwards, ethylenediamine ($\text{C}_2\text{H}_8\text{N}_2$) (0.25 ml, 2 mmol) dissolved in a mixture of water (10 mL) and ethanol (10mL) was added to the resulting reaction mixture leading to final pH 5.5, then the solution is stirred for 30 min and filtered. The filtrate was allowed to evaporate at room temperature. Yellow orange block crystals of *EnV2W4* were obtained within 10 days (yield: 65% based on W). Anal. Calc. for $\text{C}_4\text{H}_{24}\text{N}_4\text{V}_2\text{W}_4\text{O}_{21}$: H 1.84, C 3.68, N 4.3, V 7.83, W 56.49%; Found: H 1.78, C 3.55, N 4.25, V 7.71, W 54.51%. IR ($400\text{--}4000\text{ cm}^{-1}$): 442(s), 587(sh), 781(w), 935(w), 9523(sh), 966(w), 992 (s), 1074 (w), 1248 (m), 1335 (m), 1422 (m), 1590 (m), 2944 (m), 3135 (m), 3208(s) cm^{-1} .

Synthesis of ImV4W9

With the same way, an attempt to prepare a Lindqvist type-complex with imidazolinium cation, led us to the $[\text{V}_4\text{W}_9\text{O}_{40}]^{6-}$ Keggin form complex which is obtained accidentally in high yields by acidification of concentrated $\text{V}_2\text{W}_4\text{O}_{19}^{4-}$ as-synthesized solution. This has been previously cited by Flynn and Pope [23]. In fact, a solution of 1.32 g of $\text{Na}_2\text{WO}_4\cdot 2\text{H}_2\text{O}$ (4 mmol) and V_2O_5 (0.18 g, 1 mmol) in 100 ml was prepared and stirred at 70°C within 30 min. Then, 0.13 g of imidazole (2 mmol) was dissolved in water (20 ml) and added to the mixture. The pH was remained at

2.5 with 4M HCl solution. The resultant solution was heated again at 70 °C for 2 hours. After 20 days of evaporation at room temperature, Orange red crystals of *ImV4W9* have been obtained. Anal. Calc. for C₁₈H₃₀N₁₂O₄₀V₄W₉: H 1.03, C 7.41, N 5.76, V 6.99, W 56.8%; Found: H 1.01, C 7.38, N 5.63, V 7.71 W 55.42%. IR (400–4000 cm⁻¹): 503(s), 616(sh), 782(s), 846(sh) , 957 (s), 1051 (w), 1086 (w), 1201 (m), 1324 (m), 1437 (m), 1594 (m), 1647 (m), 2948 (m), 3166(s), 3227(m), 3555(m) cm⁻¹.

X-ray diffraction

The powder diffraction patterns were obtained using a D8 Advance Bruker powder diffractometer with CuKa ($\lambda = 1.5418 \text{ \AA}$) radiation. The crystal structures were determined from the single crystal X-ray diffraction data obtained with a Nonius Kappa CCD diffractometer (Graphite monochromated, MoK α = 0.71073). The data were collected at 23°C and the crystal data are given in Table 1. The structures were solved by direct methods using the program SHELXS-97 [24] and refined on F^2 by full matrix least squares method using SHELXL-97 [25] in the WINGX [26, 27]. All non-hydrogen atoms were refined isotropically and then anisotropically. All hydrogen atoms were placed geometrically and treated as riding in geometrically optimized positions. Water H atoms were refined using restraints [O-H = 0.85 (1) Å, H...H = 1.44 (2) Å and Uiso(H) = 1.5 Ueq(O)]. Further details of structural refinement and crystallographic data of *EnV2W4* and *ImV4W9* are given in **Table 1**. Complete crystallographic data for the structural analysis have been deposited with the Cambridge Crystallographic Data Centre (CCDC). These data can be obtained free of charge via www.ccdc.cam.ac.uk/conts/retrieving.html (or from the Cambridge Crystallographic Data Centre, 12 Union Road, Cambridge CB2 1EZ, UK).

Table 1 Crystallographic data and structure refinement parameters for *ImV4W9* and *EnV2W4*

Cristal data of <i>ImV4W9</i>		Cristal data of <i>EnV2W4</i>	
CCDC	1027162	CCDC	1027161
Formula	(C ₃ N ₂ H ₅) ₆ [V ₄ W ₉ O ₄₀]	Formula	(C ₂ N ₂ H ₁₀) ₂ [V ₂ W ₄ O ₁₉].2H ₂ O
FW	2912.95	FW	1301.55
Crystal system	Triclinic	Crystal system	Monoclinic
Space group	P1	Space group	P2 ₁ /c
a (Å)	10.297 (5)	a(Å)	8.9425 (6)
b (Å)	12.015 (5)	b (Å)	8.4976 (6)
c (Å)	21.231 (5)	c (Å)	15.2116 (11)
α (°)	83.205 (5)	β (°)	90.640 (3)
β (°)	83.788 (5)	Volume (Å ³)	1155.85 (14)
γ (°)	82.980 (5)	Z	2
Volume (Å ³)	2576.9 (18)	Dx (Mg m ⁻³)	3.740
Z	2	Crystal size (mm ³)	0.30 × 0.21 × 0.16
Dx (Mg m ⁻³)	3.754	Radiation (Å)	Mo K α 0.71073
Crystal size (mm ³)	0.29 × 0.13 × 0.06	Theta min-max (°)	3.3 - 35.2
Radiation (Å)	Mo K α 0.71073	Tot., uniq. Data, R(int)	4972 (0.019)
Theta min-max (°)	1.0 - 36.5	Observed data [I > 2.0 sigma(I)]	4556
Tot., uniq. Data, R(int)	24501(0.027)	Npar	169
Observed data [I > 2.0 sigma(I)]	15744	R, wR ₂ , S	0.080, 0.218, 1.07
Npar	694	Min. and max. resid. dens. (e/Å ³)	-6.57, 5.88
R, wR ₂ , S	0.108, 0.350, 1.15		
Min. and max. resid. dens. (e/ Å ³)	-9.45, 7.77		

Antibacterial Activity

The antibacterial experiments were performed following the modified methodology published in [28, 29]. In fact, a suspension of the tested bacteria (*Escherichia coli* ATCC 8739 G(-), *Salmonella typhimurium* ATCC 14028 G(-), *Staphylococcus aureus* ATCC 6538 G(+), *Enterococcus faecium* ATCC 19434 G(+), *Streptocoque B* (*Streptococcus agalactiae*) G(+) and *Candida albicans* ATCC 10231) was extended on the appropriate solid media plates and incubated overnight at 37°C. After 1 day, 4–5 loops of pure colonies were conveyed to saline solution in a test tube for each bacterial strain and adjusted to the 0.5 Mc Farland turbidity standard (~10⁸ cells/mL). Sterile cotton dipped into the bacterial suspension and the agar plates were streaked three times, each time turning the plate at a 60 angle and finally rubbing the swab through the edge of the plate. Sterile paper discs (Glass Microfibre filters, Whatman; 6 mm in diameter) were placed onto inoculated plates and impregnated with the diluted solutions in sterile water. Ampicillin (10 µg/mL) was used as positive control for all strains. Inoculated plates with discs were placed in a 37°C incubator. After 24 h of incubation, the results were recorded by measuring the zones of growth inhibition surrounding the disc. Clear inhibition zones around the discs indicated the presence of antimicrobial activity.

Results and Discussion

ICP and elemental analysis

The composition of *EnV2W4* and *ImV4W9* compounds are determined by elemental and ICP analysis. The ICP analyses indicate the presence of four vanadium atoms along with nine tungsten atoms in the cluster anion in compound *ImV4W9* and two vanadium atoms along with four tungsten atoms in polyoxoanion in compound *EnV2W4*. The wt. % of compounds *ImV4W9* and *EnV2W4* (Table 2) confirm that the two clusters can be formulated respectively as [V₄W₉O₄₀]⁶⁻ and [V₂W₄O₁₉]⁴⁻. The CHN elemental analyses confirm so the chemical formulae (C₃N₂H₅)₆[V₄W₉O₄₀] and (C₂N₂H₁₀)₂[V₂W₄O₁₉].2H₂O in terms of 4:9 ratio of V:W for *ImV4W9* and 2:4 ratio of V:W for *EnV2W4* (Table 2).

Table 2 Chemical composition (wt. %) of ImV4W9 and EnV2W4 by ICP and elemental analyses

	Experimental wt.% of elements						calculated wt.% of elements				
	V	W	C	N	H		V	W	C	N	H
(C ₃ N ₂ H ₅) ₆ [V ₄ W ₉ O ₄₀]	5.97	55.42	7.38	5.63	1.01		6.99	56.8	7.41	5.76	1.03
(C ₂ N ₂ H ₁₀) ₂ [V ₂ W ₄ O ₁₉].2H ₂ O	7.71	54.51	3.55	4.25	1.78		7.83	56.49	3.68	4.3	1.84

Powder X-ray analysis of EnV2W4 and ImV4W9

The crystallinity and purity of title compounds were confirmed by superposition of their experimental powder diffraction patterns with the calculated ones (Figure 1) exposing so good correlation. In addition, it is noted that the presence of the typical reflexions at 8° <2θ <10° in the powder pattern of *ImV4W9*, well prove that this later possesses the so-called Keggin structure [10, 30-32].

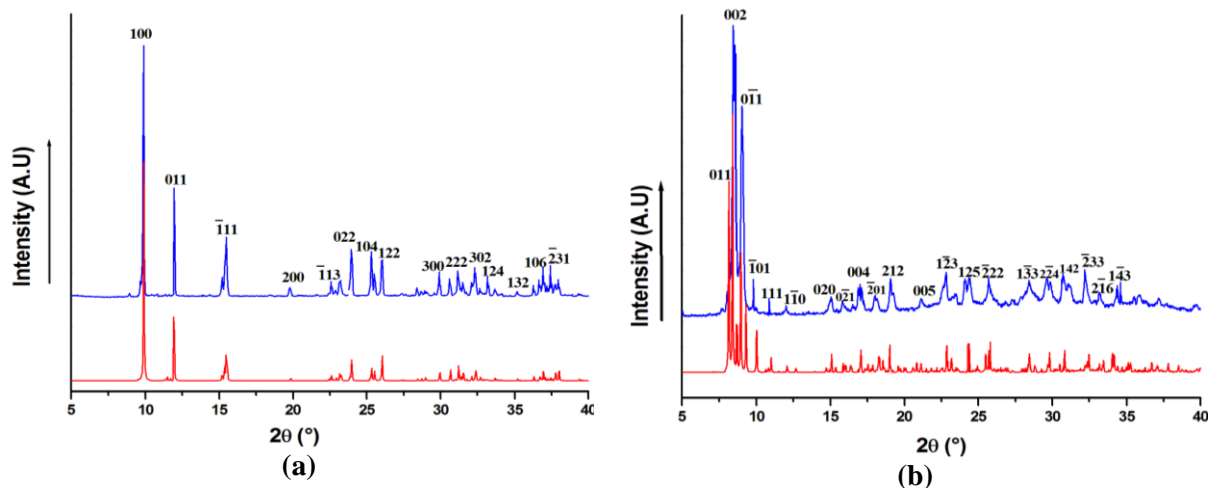


Figure 1 Experimental (blue) and theoretical (red) powder X-ray diffraction patterns of (a) EnV2W4 and (b) ImV4W9

Structure of EnV2W4

The molecular asymmetric unit of *EnV2W4* consists of one $[C_2H_{10}N_2]^{2+}$ diprotonated cation, a half of $[V_2W_4O_{19}]^{4-}$ as lying on an inversion centre and one lattice water molecule as shown in **Figure 2a**. It is noted that the crystallographical positions of the two vanadium atoms are completely disordered in the whole Lindqvist $[V_2W_4O_{19}]^{4-}$ cluster just as the same as the antecedently reported materials [19-21, 33-35]; each metal site is occupied by 1/3 V and 2/3 W. The polyoxidoanion $[V_2W_4O_{19}]^{4-}$ which is iso-structural with $[M_6O_{19}]^{2-}$, the so-called Lindqvist kind isopolyanion, consists of six MO_6 (with M = W/V) metal-oxygen octahedral with edge-sharing oxygen atoms (**Figure 2b**). The M—O bond distances are classified in three groups depending on the type of oxygen atoms; M—O_E, M—O_b and M—O_C (with O_E: terminal oxygen atoms, O_b: bridging μ_2 -oxygen atoms of type M—O_b—M and O_C: central μ_6 -oxygen atom) respectively ranging [1.646 (10) - 1.687 (11) Å], [1.879 (9) - 1.966 (9) Å] and [2.2769 (6) - 2.3156 (5) Å]. The M—O—M bond angles vary from 75.5 (2) ° to 178.5 (4) °. These values indicate a distorted octahedral geometry around the tungsten/vanadium atoms confirmed by the calculated distortion indexes [36] of M1O₆ (0.357), M2O₆ (0.335), M3O₆ (0.392).

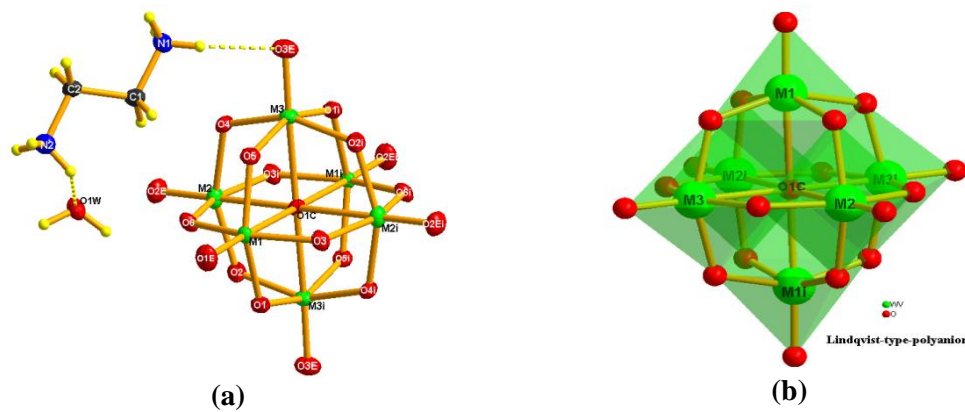


Figure 2 (a) ORTEP diagram of EnV2W4 (b) Polyhedral views of the $[V_2W_4O_{19}]^{4-}$ polyoxidoanion (M = W/V)

The crystal packing of *EnV2W4* shows that the anionic subunits align into chains; $\{[V_2W_4O_{19}(H_2O)_2]^{4-}\}_n$ along [100] direction thanks to water molecules via moderate O1W—H...O hydrogen bonds with O1W...O distances varying from 2.694(12) to 3.344(13) Å (**Table 3, Figure 3**).

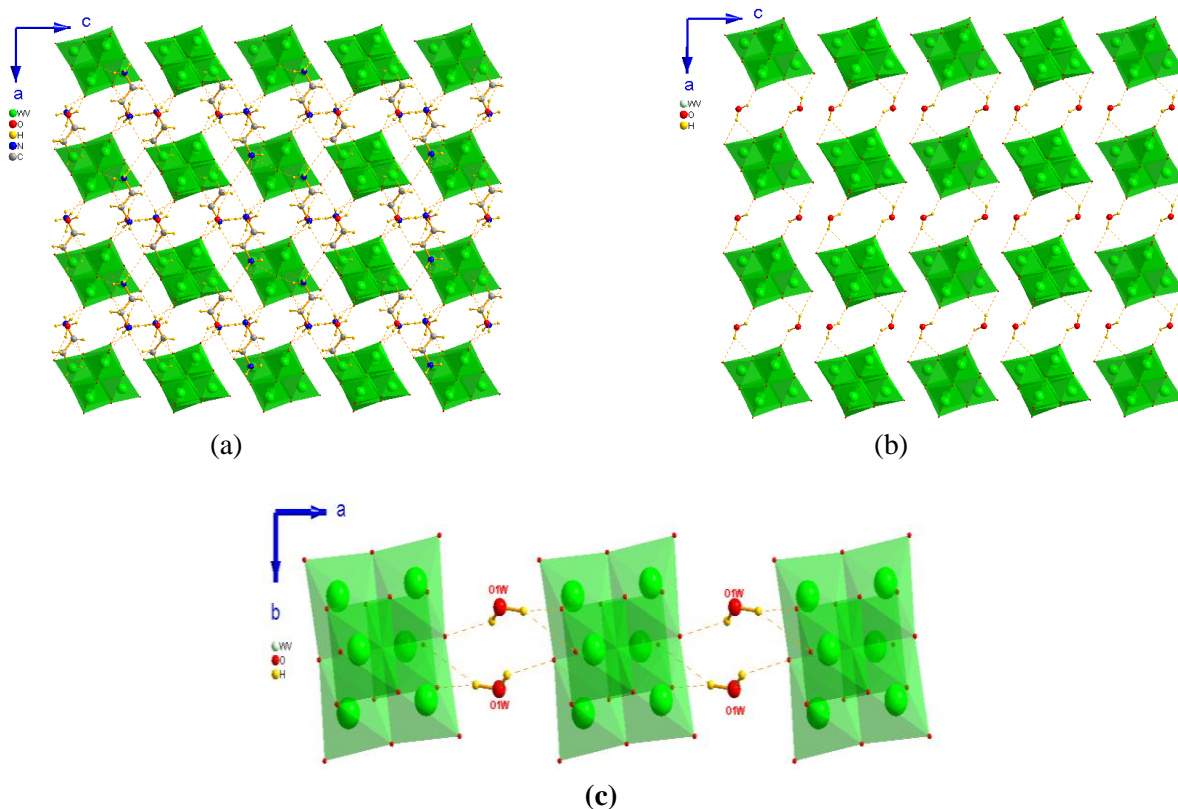


Figure 3 (a) Crystal packing of EnV2W4 along b axis, (b) A view along b axis of $\{[V_2W_4O_{19}(H_2O)_2]^{4-}\}_n$ chains
 (c) 1D-anionic framework aligned along a axis

As every cluster anion is surrounded by six counterions with helical manner of approximately diameter of 12 Å; the encapsulated $\{[V_2W_4O_{19}(H_2O)_2]^{4-}\}_n$ chains are extended into 1D helical-like channels, as shown in Figure 4.

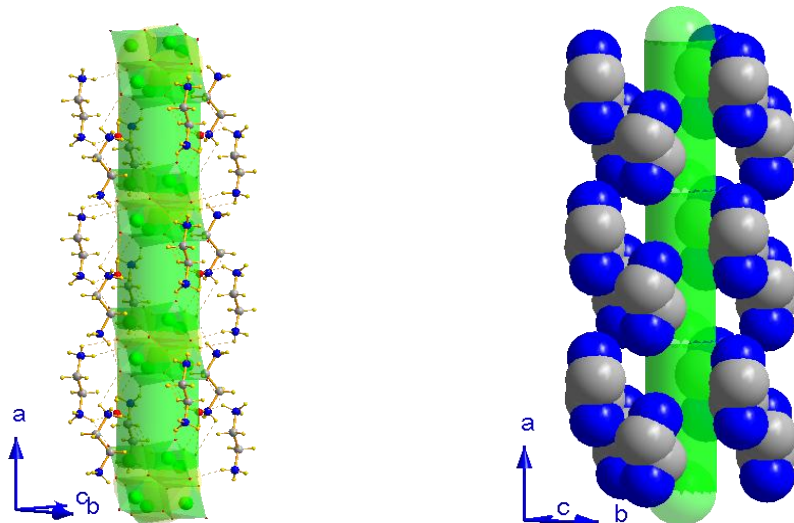


Figure 4 (a) Space-fill and (b) ball-stick representation of the 1D helical-like channels in EnV2W4.

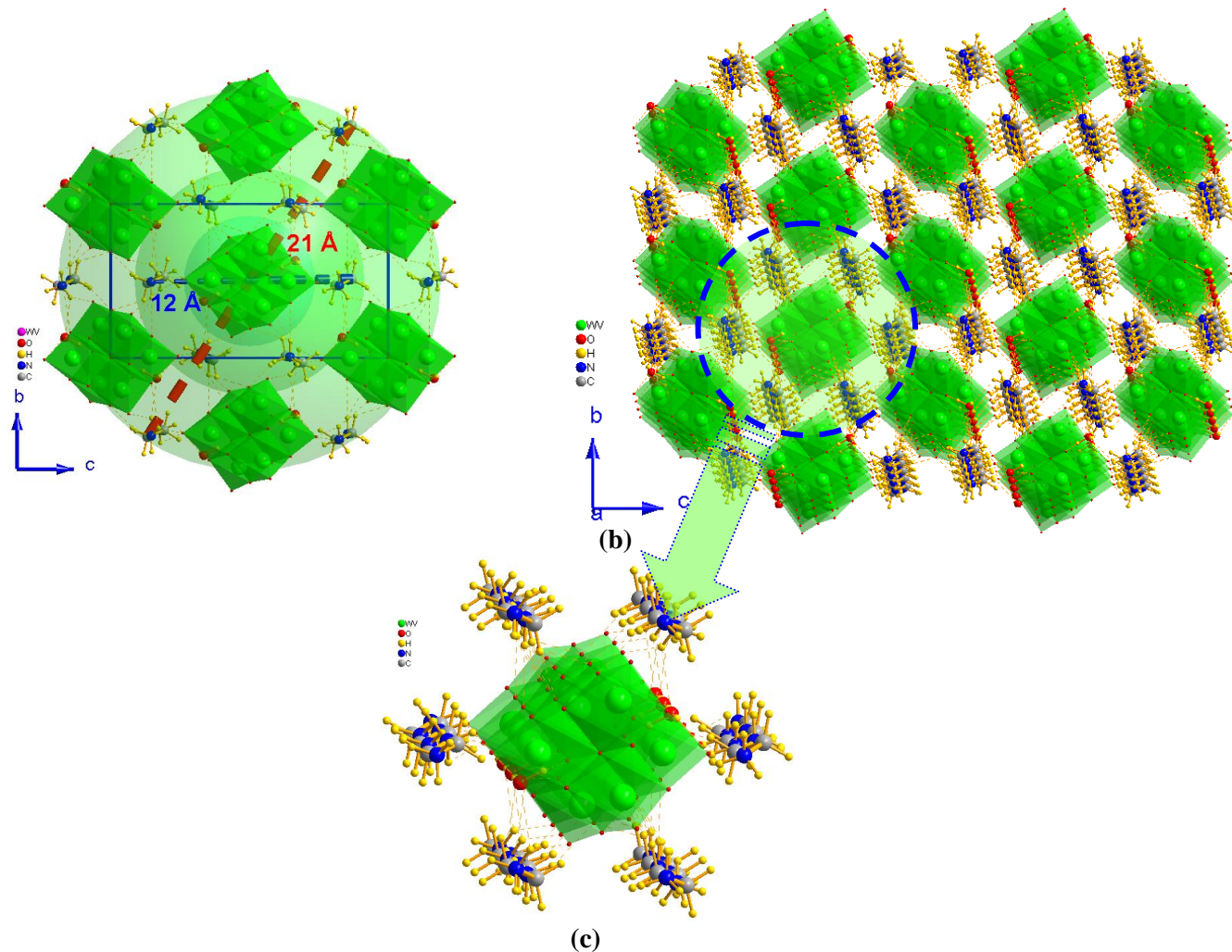


Figure 5 (a) 1D sphere-like channels forming by alternation between inorganic chains and organic cations
(b) Perspective view of 3D-supramolecular network of EnV2W4 (c) Hydrogen bond scheme around $\{[V_2W_4O_{19}(H_2O)_2]^{4-}\}_n$ chain

These channels are also enveloped by means six alternating $\{[V_2W_4O_{19}(H_2O)_2]^{4-}\}_n$ chains and diprotonated cations in sphere of $\sim 21 \text{ \AA}$ (**Figure 5a**) to complete a 3D-supramolecular network (**Figure 5b**). With regard to organic moieties, the ethylenediammonium cation adopts an extended conformation with a N—C—C—N torsion angle of 177.63° resulting in an overall helical arrangement of the $[H_3NCH_2CH_2NH_3]^{2+}$ cations and $[V_2W_4O_{19}]^{4-}$ polyanions which are extensively bonded through N—H...O hydrogen bonds (**Figure 5c**) with N...O distances ranging from $2.857(14)$ to $3.365(15) \text{ \AA}$ (**Table 3**). It is noted that The C—C and C—N bond lengths are similar to those reported in related compound such as $(C_2H_{10}N_2)_3(C_2H_9N_2)_2[Mo_5(HPO_4)_2O_{15}] \cdot 10H_2O$ and $(C_2H_{10}N_2)[Mo_3O_{10}]$ [37-38].

Table 3 Hydrogen-bond geometry (\AA , $^\circ$) of EnV2W4

D—H...A	D—H	H...A	D...A	D—H...A
O1W—H1W1...O3E ⁱⁱ	0.91 (2)	2.50(2)	3.344(13)	155(6)
O1W—H1W1...O1 ⁱⁱⁱ	0.91 (2)	2.07(3)	2.694(12)	124(4)

O1W—H2W1···O6	0.89 (3)	2.00(8)	2.706(12)	136(11)
N1—H1A···O2 ^{iv}	0.89	2.25	2.935(15)	134
N1—H1A···O5 ^v	0.89	2.53	3.365(15)	156
N1—H1B···O3E	0.89	2.30	3.067(15)	145
N1—H1B···O4 ^{vi}	0.89	2.57	3.149(15)	124
N1—H1C···O3 ^{vii}	0.89	2.07	2.852(14)	147
N2—H2A···O1W	0.89	2.31	2.794(15)	114
N2—H2B···O1E ^{viii}	0.89	2.26	2.931(15)	132
N2—H2B···O3E ⁱⁱ	0.89	2.55	2.984(15)	111
N2—H2C···O2E ^{ix}	0.89	2.13	2.857(14)	138
N2—H2C···O1W ^{ix}	0.89	2.31	2.870(16)	121
C2—H2E···O2 ^{iv}	0.97	2.39	3.166(15)	137

Symmetry codes: (ii) $x-1, y, z$; (iii) $-x, -y+1, -z+1$; (iv) $x, -y+3/2, z+1/2$; (v) $-x+1, y+1/2, -z+3/2$; (vi) $-x+1, y-1/2, -z+3/2$; (vii) $x, -y+1/2, z+1/2$; (viii) $-x, y+1/2, -z+3/2$; (ix) $-x, y-1/2, -z+3/2$.

Structure of *ImV4W9*

Single-crystal X-ray diffraction analysis reveals that *ImV4W9* is built up from six imidazolium cations and one Keggin-type polyoxoanion $[V(V_3W_9O_{40})^{6-}]$ (**Figure 6a**) in which the central tetrahedron is occupied by V^V; whereas 3 V atoms and 9 W atoms are positionally disordered over the whole V-substituted Keggin polyanion, $[VM_{12}O_{40}]^{n-}$ in which each metal M (with M = W/V) site was assigned as 9/12W and 3/12 V. Furthermore; the BVS results verify that the central vanadium atom has +V oxidation state (4.9964 valence unit) [39].

The $[V(V_3W_9O_{40})^{6-}]$ anion exhibits the renowned α -Keggin-type structure. It may be described as a shell of $\{M_{12}O_{36}\}$ (M = W/V) encapsulating a $\{VO_4\}$ central tetrahedron corner-sharing four triad $\{M_3O_{13}\}$ cluster (**Figure 6b**). Each oxygen of the VO_4 core is covalently bonded to three different metal centers so it is characterized by μ_4 -bridging mode with V1C—O_{μ4} bond distances and angles ranges are respectively 1.518(10) – 1.582(11) Å and 106.4(6)–112.3(6) $^{\circ}$. The average V1C—O distances [1.541 Å] is comparable to the corresponding bond distance [1.538(10) Å] in the fully oxidized Keggin-like isopolyvanadate $[V_{15}O_{42}]^{19-}$ [40-41] confirming the (+V) oxidation state of V1C which corroborates with the analysis results. These geometric features reveal that the tetrahedron around the vanadium center is slightly distorted. The shell is constructed from a total of twelve MO_6 octahedra with M—O bond lengths of M—O_t: 1.631(18) – 1.716(11) Å; M—O_{μ2}: 1.854(2) – 1.954(13) Å and M—O_{μ4}: 2.360(11) – 2.476(12) Å (with O_t: terminal oxygen atoms of type M—O_t, O_{μ2}: bridging oxygen atoms of type M—O_{μ2}—M and O_{μ4}: bridging oxygen atoms of type M—O_{μ4}—V1C) and M—O—M bond angles ranging from 70.8(4) to 159.2(4) $^{\circ}$. These geometrical characteristics are analogous to those observed in related structure of V-substituted Keggin type clusters [11, 42-43]. It's to be noted the considerable distortion observed inside MO_6 octahedra (ID($M1O_6$) = 0.357, ID($M2O_6$) = 0.337, ID($M3O_6$) = 0.392, ID($M4O_6$) = 0.388, ID($M5O_6$) = 0.382, ID($M6O_6$) = 0.350, ID($M7O_6$) = 0.397, ID($M8O_6$) = 0.337, ID($M9O_6$) = 0.343, ID($M10O_6$) = 0.39 ID($M11O_6$) = 0.42 and ID($M12O_6$) = with ID = distortion indexes).

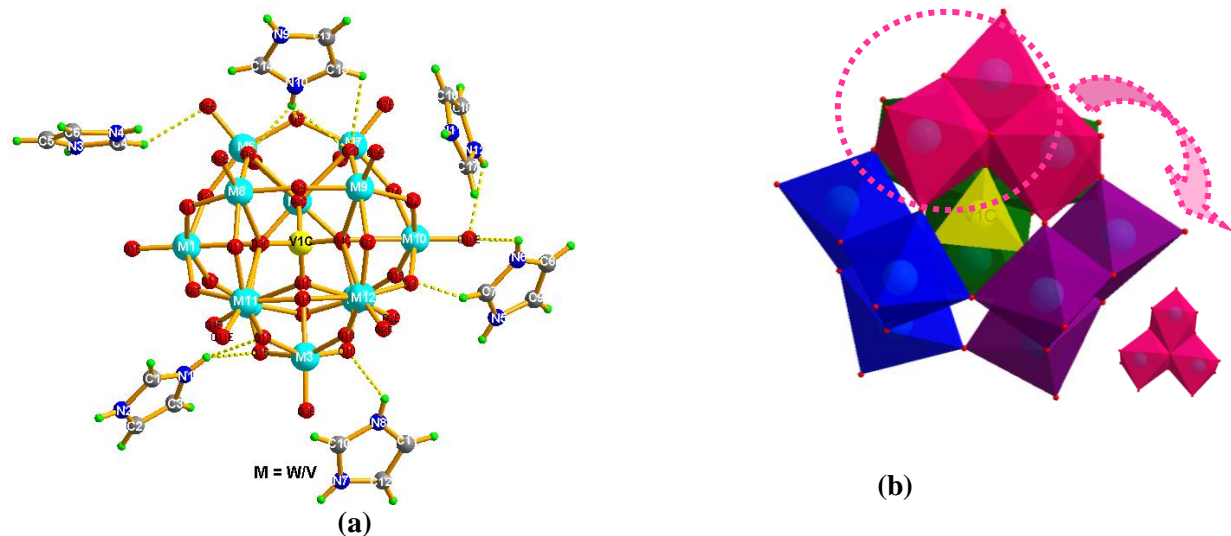


Figure 6 (a) The molecular structure of *ImV4W9* (b) Polyhedral views of the $[VM_{12}O_{40}]^{6-}$ polyoxoanion and the trimetallic $\{M_3O_{13}\}$ subunits with $M = W/V$.

In the crystal packing of *ImV4W9*, the $[V(V_3W_9)O_{40}]^{6-}$ Keggin anions and imidazolinium cations self-assemble into a hybrid host three dimensional network (**Figure 7**).

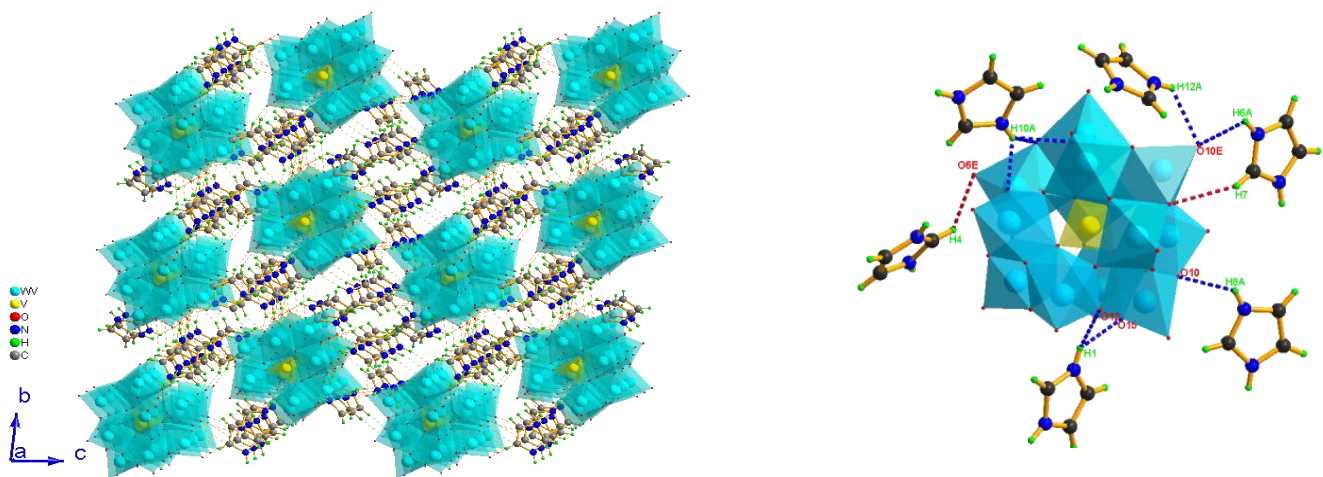


Figure 7 (a) The packing of the 3D-supramolecular network of *ImV4W9* in perspective view and (b) N—H...O and C—H...O intermolecular interactions in the structure of *ImV4W9*

As shown in **Figure 7b** each Keggin structure connects to six neighboring imidazolinium moieties involving a set of hydrogen bonds. In fact; the protonated cation and $[V(V_3W_9)O_{40}]^{6-}$ cluster anions are in a shut connection through strong N—H...O hydrogen bonds with N...O distances ranging between 2.50 (3) and 3.32 (2) Å (Table 4). As well, the C—H...O interactions are also appearing with C...O distances varying from 2.65(2) to 3.46(3) Å (Table 4) giving rise to a 3D grid-like network (Figure 7a). Additionally, anionic clusters and *ImH⁺* cations assemble into a porous 3-D hydrogen-bonded host framework in which the independent cations reside in the channel voids balancing charge and participating in the extensive hydrogen-bonding 3D-supramolecular network (**Figure 8**).

With regard to organic moieties, the imidazolium rings are basically planar with mean deviation from least-square plane is ± 0.005 Å. This cations interact with each other via dispersion interactions, including a C—H \cdots π contacts to imidazole rings with distance of 2.76 Å between H6 and Cg₅ (centroid of (N9—N10) ring). As well, a significant $\pi\cdots\pi$ stacking interactions with short separation of 3.684 Å between Cg₁ and Cg₃ respectively the centroids of (N1—N2) and (N5—N6) rings, have been also detected (**Figure 9**).

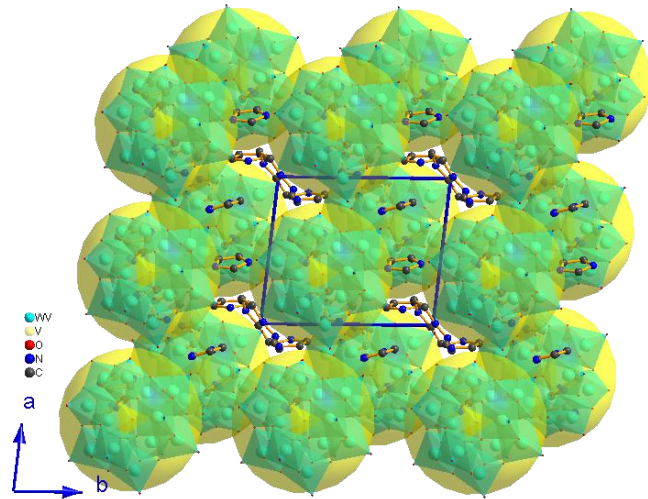


Figure 8 A porous 3-D supramolecular network of ImV4W9 viewed along c-axis

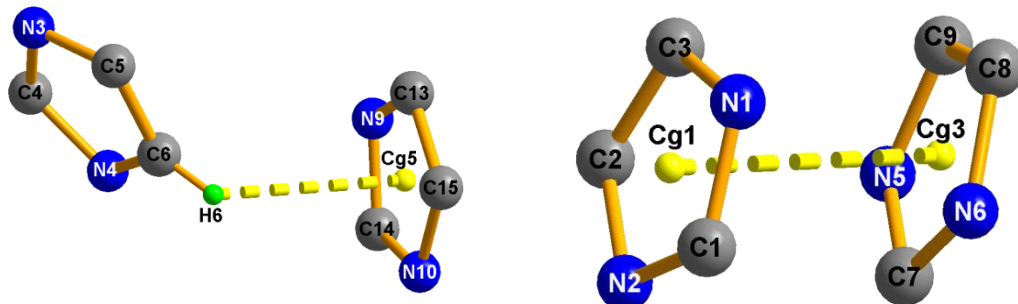


Figure 9 C—H \cdots π and $\pi\cdots\pi$ interactions between neighboring imidazole rings

Table 4 Hydrogen-bond geometry (Å, °) of ImV4W9

D—H \cdots A	D—H	H \cdots A	D \cdots A	D—H \cdots A
N1—H1 \cdots O15	0.86	2.18	2.803 (13)	129
N1—H1 \cdots O12	0.86	2.19	2.941 (16)	145
N1—H1 \cdots O21	0.86	2.61	3.046 (16)	113
N1—H1 \cdots O17	0.86	2.66	3.220 (16)	124
N2—H2 \cdots O6 ⁱ	0.86	2.00	2.775 (13)	150

N2—H2···O24 ⁱ	0.86	2.37	2.911 (16)	121
N2—H2···O4 ⁱ	0.86	2.38	2.878 (14)	117
N3—H3A···O13 ⁱⁱ	0.86	2.19	2.920 (18)	142
N3—H3A···O14 ⁱⁱ	0.86	2.37	3.09 (2)	141
N4—H4A···O8E ⁱⁱⁱ	0.86	2.03	2.716 (18)	137
N5—H5A···O5E ^{iv}	0.86	2.16	2.95 (2)	152
N6—H6A···O10E	0.86	2.50	3.07 (2)	125
N7—H7A···O12E ^v	0.86	1.96	2.66 (2)	137
N7—H7A···O17 ^{vi}	0.86	2.57	3.25 (3)	136
N7—H7A···O1E ^{vi}	0.86	2.60	3.03 (3)	112
N8—H8A···O10	0.86	2.42	3.09 (4)	136
N8—H8A···O2E	0.86	2.65	3.29 (3)	132
N9—H9A···O1E ⁱⁱⁱ	0.86	2.53	3.32 (2)	152
N10—H10A···O8	0.86	2.03	2.69 (3)	132
N10—H10A···O5	0.86	2.10	2.84 (3)	145
N10—H10A···O20	0.86	2.30	2.77 (3)	114
N11—H11A···O9E	0.86	2.20	2.50 (3)	100
N12—H12A···O10E	0.86	2.40	2.97 (2)	124

Symmetry codes: (i) x, y−1, z; (ii) x−1, y, z; (iii) −x+1, −y+1, −z+1; (iv) −x+1,

Infrared spectroscopy

The IR spectrum of *EnV2W4* is shown in **Figure 10a**. Following the vibrational analysis of Flynn and Pope [47] for $\text{V}_2\text{W}_4\text{O}_{19}^{4-}$, the asymmetric stretching mode for the terminal M=O_t groups should be splitting into four bands in the IR-spectrum between 991 and 930 cm^{−1}, instead of one band at 978 cm^{−1} of nearly pure mode of W=O_t for $\text{W}_6\text{O}_{19}^{2-}$. With regard to IR spectrum of *EnV2W4*, it exhibits characteristic bands at 992, 966, 953 and 935 cm^{−1}; well confirm the 2:4 Lindquist-type cluster $\text{V}_2\text{W}_4\text{O}_{19}^{4-}$. The symmetric and asymmetric stretching vibration of (M—O_b) are respectively observed at 778 cm^{−1}, 587 and 422 cm^{−1} as earlier evidenced [19-22, 44-47]. The bands appearing at 3135, 2944, 1590, 1422, 1335, 1248 and 1074 cm^{−1}, are characteristic absorption of ethylenediammonium cation [48-50]. The broad bands at 3204 and 1622 cm^{−1} are ascribed to vibrations of (H₂O).

In the IR spectrum of *ImV4W9* (**Figure 10b**), the bands observed at 957, 846 are attributed to v (M—O_{μ2}—M) and v (M—O_{μ4}—M) of polyanion. The strong absorption at 782 cm^{−1} is due to the stretching vibration of the central tetrahedral (VO₄) [51] whereas those appearing at 1086 and 1051 cm^{−1} are respectively assigned to the asymmetric and symmetric vibrations of V=O_t, characteristics of the tri-vanadium-substituted Keggin type heteropolyanion as well as previously cited in literature [17,52- 53]. Features at 1647, 1590 and 1429 cm^{−1} were assigned to the bending v (NH) vibration coupled with the v (C=C) and v (C=N) stretching vibrations where those at 3227, 3149 and 2957 cm^{−1} are allocated to the v (C—H) and v(N—H) stretching vibrations of the imidazolinium moiety [54, 55].

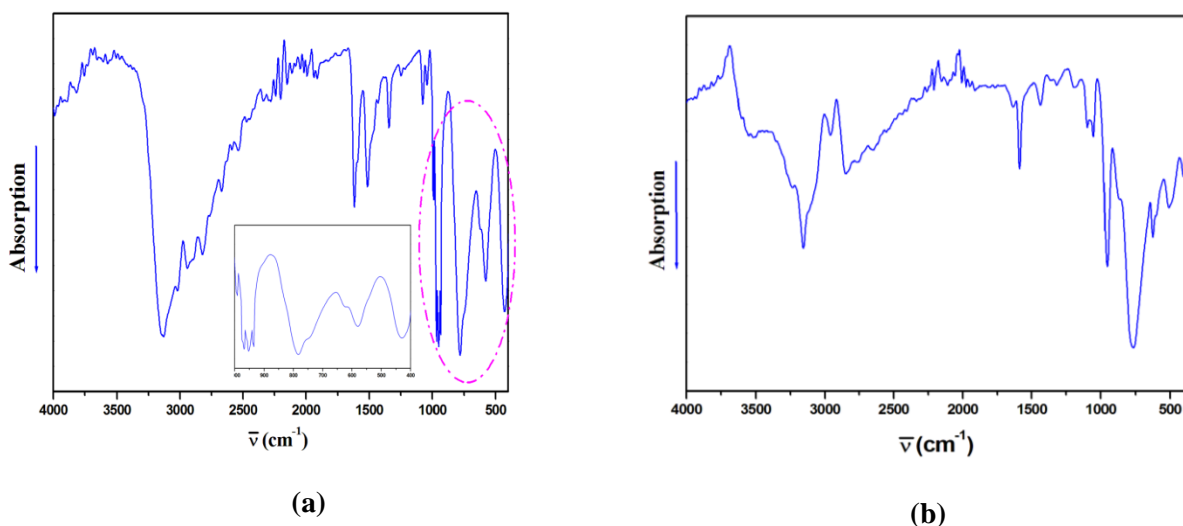


Figure 10 IR spectra of (a) EnV2W4 and (b) ImV4W9.

TG analysis

The TG curve (**Figure 11a**) for *EnV2W4* compound shows a first weight loss of 2.8% in the temperature range of 98–190 °C. This weight loss is due to the loss of two water molecules (2.77 % calculated). The second weight loss of 9.17 % observed between 250 and 500 °C was primarily ascribed to the decomposition of ethylenediammonium cations (9.52 % calculated) [56–57]. The third weight loss in the temperature range of 500–800 °C may be allocated to the pyrolysis of the residual material leading to metal oxides [47].

The TG curve of *ImV4W9* is depicted in **Figure 11b**. It shows that there is no any weight loss below 200°C indicating that sample was free of water which is in good agreement with structural model and the results of FT-IR spectroscopy. The thermal analysis exhibits two step processes. A first weight loss of 14.66 % between 300 and 470 °C is ascribed to the decomposition of the organic moieties in concordance with the calculated weight loss 14.22 %. The second weight loss extending to 600°C can be assigned to the collapse of the Keggin structure leading to of metal oxides [58-59].

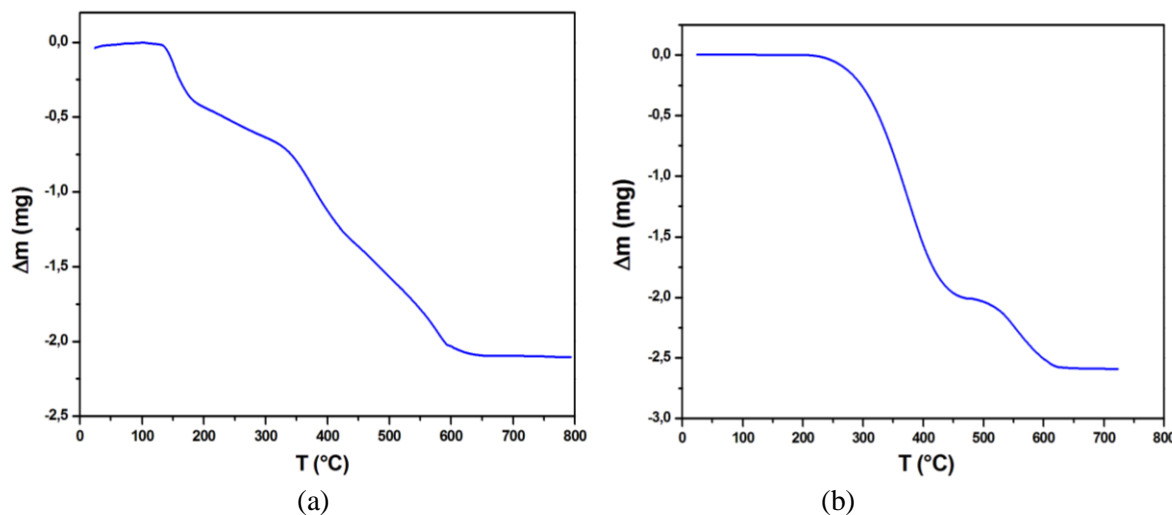


Figure 11 TG thermograms of (a) EnV2W4 and (b) ImV4W9

UV-Vis spectra and optical band gap

The electronic spectrum of *EnV2W4* is shown in **Figure 12a**. It displays a broad band centered at 391 nm which can be referred to charge transfer (LMCT) transitions of O→V/W, as mentioned in the previous literature for $[V_2W_4O_{19}]^4-$ cluster containing compounds [54,60-61].

The UV-Vis electronic spectra of *ImV4W9* and pure imidazole in solid state are given in **Figure 12b**. The spectrum of the complex exhibits a broad band extending to 500 nm in visible range, with maxima centered at 252 nm and 360 nm which could be assigned to $\pi \square \pi^*$ transition of imidazole ring as compared to absorption band of pure imidazole (**Figure 12b**) and also to ligand-to-metal charge-transfer (LMCT) transitions of the O→V/W [62-64]. In addition, solid state electronic absorption (diffused reflectance) spectra provided by using the Tauc model [65] the optical band gaps of ca. 3.95 and 2.9 eV respectively for *ImV4W9* and *EnV2W4* as reported in **Figure 12** well mentioned the semiconductor behavior of these materials [66-68].

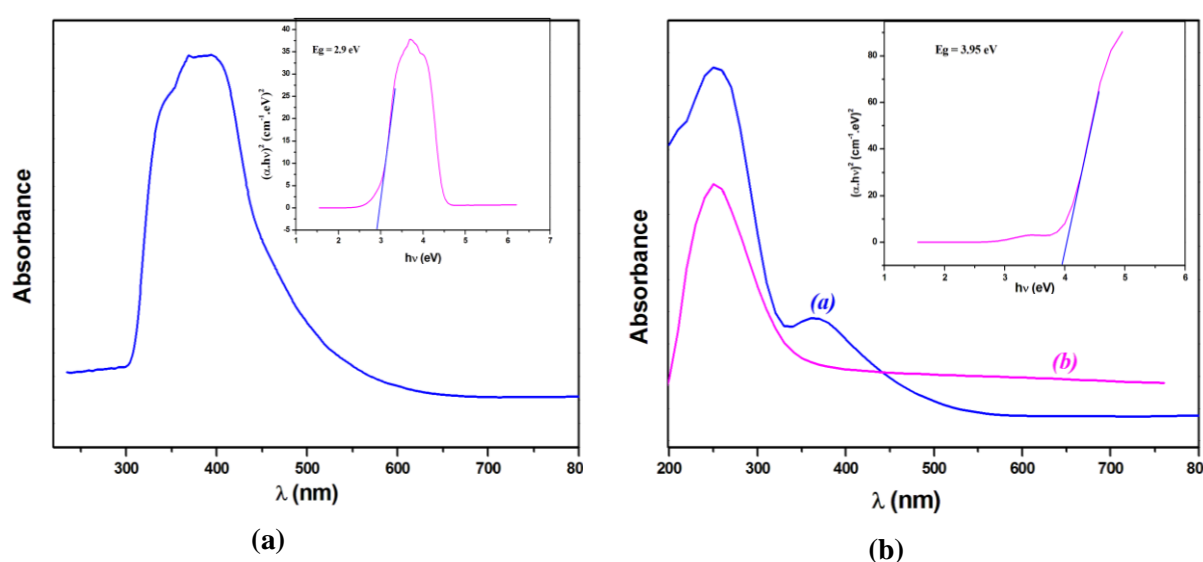


Figure 12 Solid state electronic spectra and energy gap determinations of (a) *EnV2W4* and (b) *ImV4W9*

Photoluminescent property

The emission spectrum of *EnV2W4* upon excitation at *ca.* 350 nm is shown in Figure 13a. The PL spectrum displays a strong blue emission at about 476 nm and two weakened fluorescence bands at 400 and 543 nm. This photoluminescence effect is due to charge transfer of O→V/W as evidenced by UV-visible analysis and regarded in other polyoxoanion systems [69-72].

The emission spectrum of *ImV4W9* depicted in Figure 13b, exhibits strong broad red photoluminescence band centered around *ca.* 650 nm upon excitation at 360 nm (Figure 13b) which can be referred to the charge transfer of O→M (M = W/V, V) in the $[V_4W_9O_{40}]^{6-}$ and the $\square \dots \square^*$ transitions of the imidazolinium cations [6, 63] well correlated with X-ray and UV-visible results.

The above-mentioned results indicate that both *ImV4W9* and *EnV2W4* may well be excellent candidates for potential luminescence materials.

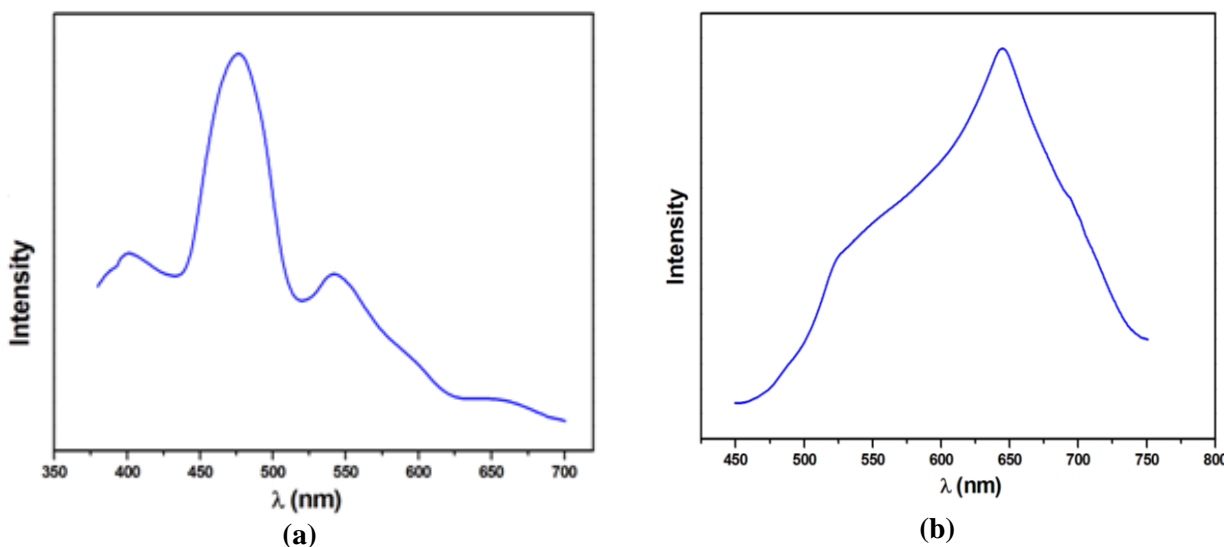


Figure 13 Emission spectra of (a) EnV₂W₄ and (b) ImV₄W₉ in the solid state.

Antibacterial Activity of EnV₂W₄ and ImV₄W₉

Determination of the antimicrobial activities of the new compounds and their initial reactants was carried out *in vitro* by the agar well diffusion method against six bacteria, *Escherichia coli* ATCC 8739 G(-), *Salmonella typhimurium* ATCC 14028 G(-), *Staphylococcus aureus* ATCC 6538 G(+), *Enterococcus faecium* ATCC 19434 G(+), *Streptocoque B* (*Streptococcus agalactiae*) G(+) and *Candida albicans* ATCC 10231. In the Preliminary studies, these tests were judged by measuring the inhibition zone growth diameter (IZD) for graded concentrations 100, 150 and 200 $\mu\text{g/mL}$ of different samples with the results shown in **Tables 5 and 6** and displayed in the Bar diagrams in **Figure 13**. It is obvious that synthesized compounds show potent activities against the tested microorganisms with inhibition zones ranging from 7 to 11 mm.

As exposed in **Figure 13a**, The *EnV₂W₄* compound exhibits a promising ability with the maximum inhibition zone diameter observed against *C. albicans* at 200 $\mu\text{g.mL}^{-1}$. It displays a much higher antimicrobial activity versus the same tested bacteria than its basic reagents the ethylenediamine and $(\text{NH}_4)_4\text{V}_2\text{W}_4\text{O}_{19}$. In fact, the ethylenediamine and $(\text{NH}_4)_4\text{V}_2\text{W}_4\text{O}_{19}$ possess antimicrobial effect as antecedently established for some similar materials [73-77, 78-79]. In addition, the observed results reveal that antimicrobial activity of the compound is directly proportional to the concentration and the nature of bacteria. The structure of Gram negative cell walls bacteria (e.g. *E. coli*) are complex compared to Gram positive ones (e.g. *Streptocoque B*) well elucidate the robustness and resistance of Gram negative bacteria versus the tested compounds [80].

As well, *ImV₄W₉* shows significant efficacy against the six microbes in comparison with pure imidazole and $(\text{NH}_4)_6\text{V}_4\text{W}_9\text{O}_{40}$ which also owned good antibacterial activity (**Figure 13b**). The literature contains a number of reports on the antimicrobial properties of some polyoxometalates [73-77] as well as of imidazole and a number of their derivatives [81, 82]. The results gathered in **Table 6**, reveal that Gram positive *Streptocoque B* has significant effect than the other tested bacterial strains showing a maximum inhibition for concentration 200 $\mu\text{g/mL}$.

It is possible that the synergy between the highly-negative charge anions and the positively charged cations, lead to the antimicrobial enhancement process. In addition, the antibacterial properties of both compounds can be explained by electrostatic interactions occurring between the electrolytic materials and the charged surface membrane of the bacteria by blocking their replication. The extensive hydrogen-bond network featuring between species, can also participate in the mechanism of inhibition by disrupting the cell walls microbes which causes the cytoplasmic

membrane contents of the cell to leak out [83-84]. As results, both materials could have an excellent biocidal effect and effectiveness in reducing bacterial growth.

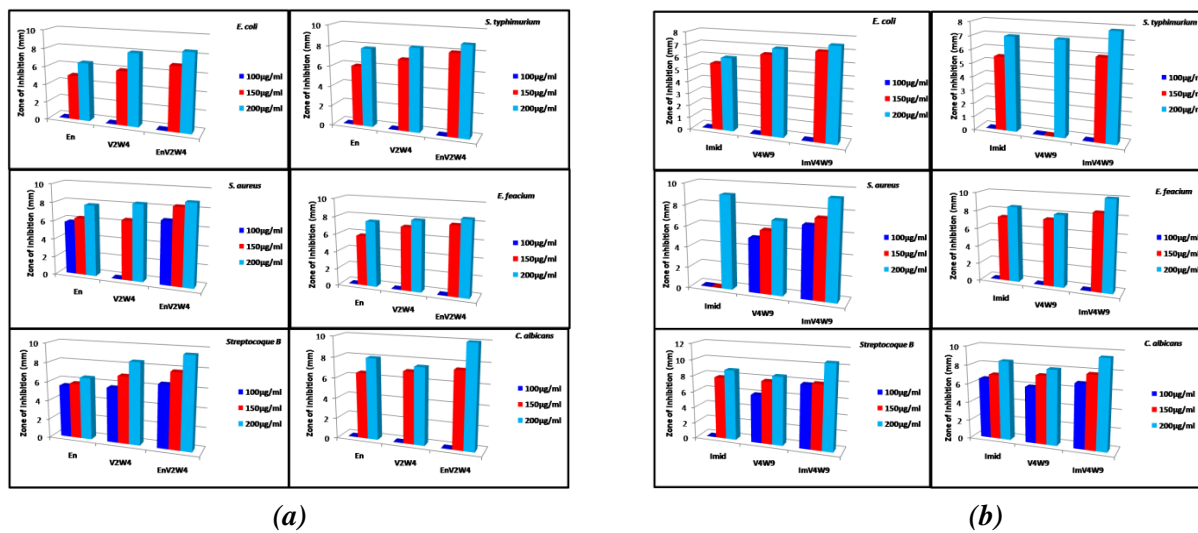


Figure 14 (a) Antimicrobial activity of En, V2W4 and EnV2W4 against six bacteria. (b) Antimicrobial activity of Imid, V4W9 and ImV4W9 against six bacteria

Table 5 Antibacterial Activity data of compound (EnV2W4), pure ethylenediamine (En) and $(\text{NH}_4)_4\text{V}_2\text{W}_4\text{O}_{19}$ (V2W4) against the selected bacteria

Inhibition Zone Diameter [mm]															
C ($\mu\text{g/mL}$)	E. Coli			S. typhimurium			S. aureus								
	En	V2W4	EnV2W4	En	V2W4	EnV2W4	En	V2W4	EnV2W4						
100	-	-	-	-	-	-	5.8 \pm 0.0	-	6.8 \pm 0.3						
150	5 \pm 0.0	6 \pm 0.0	7 \pm 0.0	6 \pm 0.0	7 \pm 0.0	8 \pm 0.0	6.3 \pm 0.5	6.5 \pm 0.7	8.3 \pm 1.0						
200	6.5 \pm 0.7	8 \pm 0.0	8.5 \pm 0.4	7.8 \pm 0.3	8.2 \pm 0.7	8.8 \pm 0.3	7.8 \pm 0.7	8.3 \pm 0.3	8.8 \pm 1.0						
Inhibition Zone Diameter [mm]															
C ($\mu\text{g/mL}$)	E. faecium			Streptococcus B			C. albicans								
	En	V2W4	EnV2W4	En	V2W4	EnV2W4	En	V2W4	EnV2W4						
100	-	-	-	5.5 \pm 0.0	5.7 \pm 0.3	6.5 \pm 0.0	-	-	-						
150	5.8 \pm 0.3	7.2 \pm 0.4	7.8 \pm 0.3	5.8 \pm 1.0	7 \pm 0.0	7.8 \pm 1.0	6.5 \pm 0.7	7 \pm 0.0	7.5 \pm 0.3						
200	7.5 \pm 0.7	8 \pm 0.0	8.5 \pm 0.7	6.5 \pm 0.7	8.5 \pm 0.7	9.5 \pm 0.7	8 \pm 0.0	7.5 \pm 0.7	10 \pm 0.0						
The antibiotic controls: Ampicilline (10 $\mu\text{g/mL}$) Zone of Inhibition [mm]															
E. Coli		S. typhimurium		S. aureus		E. faecium		Streptococcus B							
9.5 \pm 0.7		10.5 \pm 0.7		38 \pm 1.4		41 \pm 1.4		28.5 \pm 2.1							
C. albicans															
30.5 \pm 0.7															

Table 6 Antibacterial Activity data of compound (ImV4W9), pure imidazole (Imid) and $(\text{NH}_4)_6\text{V}_4\text{W}_9\text{O}_{40}$ (V4W9) against the selected bacteria

Inhibition Zone Diameter [mm]									
C ($\mu\text{g/mL}$)	E. Coli			S. typhimurium			S. aureus		
	Imid	V4W9	ImV4W9	Imid	V4W9	ImV4W9	Imid	V4W9	ImV4W9
100	-	-	-	-	-	-	-	5.2±0.2	6.8±0.3
150	5.5±0.0	6.5±0.2	7±0.0	5.5±0.0	-	6±0.0	-	6±0.0	7.5±0.7
200	6±0.0	7±0.2	7.5±0.3	7±0.0	7±0.0	7.8±0.3	9±0.0	7±0.3	9.3±0.3
Inhibition Zone Diameter [mm]									
C ($\mu\text{g/mL}$)	E. faecium			Streptocoque B			C. albicans		
	Imid	V4W9	ImV4W9	Imid	V4W9	ImV4W9	Imid	V4W9	ImV4W9
100	-	-	-	-	6±0.0	7.8±0.3	6.5±0.3	6±0.0	6.8±0.3
150	7.3±0.3	7.4±0.3	8.5±0.7	7.8±0.3	7.8±0.7	8±0.0	7±0.7	7.3±0.3	7.8±0.3
200	8.5±0.7	8±0.0	10±0.0	8.8±0.3	8.5±0.0	10.5±1.4	8.5±0.7	8±0.0	9.5±0.7
The antibiotic controls:Ampicilline (10 $\mu\text{g/mL}$) Zone of Inhibition [mm]									
E. Coli	S. typhimurium	S. aureus	E. faecium	Streptocoque B	C. albicans				
9.5±0.7	10.5±0.7	38±1.4	41±1.4	28.5±2.1	30.5±0.7				

With:

Bacteria	Abbreviated
Escherichia coli ATCC 8739 G(-)	E. Coli
Salmonella typhimurium ATCC 14028 G(-)	S. typhimurium
Staphylococcus aureus ATCC 6538 G(+)	S. aureus
Enterococcus faecium ATCC 19434 G(+)	E. faecium
Streptocoque B (Streptococcus agalactiae) G(+)	Streptocoque B
Candida albicans ATCC 10231	C. albicans

Conclusions

In summary, two novel V-substituted Lindqvist and Keggin-type heteropolytungstates decorated respectively with ethylenediammonium and imidazolinium cations, $(C_2N_2H_{10})_2[V_2W_4O_{19}] \cdot 2H_2O$ (*EnV2W4*) and $(C_3N_2H_5)_6[V_4W_9O_{40}]$ (*ImV4W9*), were synthesized and characterized. The crystal structure of both compounds show a 3D-supramolecular network supported by means electrostatic, extensive hydrogen bond and Van der Waals interactions. Moreover, the electronic results indicate the semi-conductor and photoluminescent behaviors of discussed compounds. Furthermore, both materials show potent antimicrobial efficacy against six pathogenic microbes which can make them applicable as antibacterial agents.

References

- [1] Schimanke G, Martin M, Kunert J, Vogel H, Z. Anorg. Allg. Chem. 2005, 631, 1289.
- [2] Landau MV, Vradman L, Wolfson A, Rao P M, Herskowitz M, C. R. Chem. 2005, 8, 679.
- [3] Mestl G, Top. Catal. 2006, 38, 69.
- [4] Pope M T, Heteropoly and Isopoly Oxometalates, Springer-Verlag, New York, 1983.
- [5] Pope MT, Kortz U, Encyclopedia of Inorganic and Bioinorganic Chemistry. Chichester John Wiley & Sons, 2012.
- [6] Katsoulis DE, Chem. Rev. 1998, 98, 359-387.
- [7] Shigeta S, Mori S, Kodama E, Kodama J, Takahashi K, Yamase T, Antiviral Res. 2003, 58, 265.
- [8] Hill CL, Weeks MS, Schinazi R F, J. Med. Chem. 1990, 33, 2767.
- [9] Shigeta S, Mori S, Wantabe J, Baba M, Khonkin AM, Hill C L, Schizazi RT, Antiviral Chem. Chemother 1995, 6, 114.
- [10] Soussi I, Aoun S, Planchat A, Akriche S, j.a.c. 2014, 10, 2182.
- [11] Hajsaalem A, Aoun S, Planchat A, Rzaigui M, Toumi SA, Acta Cryst. 2014, E70, m125.
- [12] Ueda T, Nambu J., Lu J, Guo SX, Li Q., Boas JF, Martin LL, Bond AM, Dalton Trans., 2014, 43, 5462.
- [13] Uehara K, Taketsugu T, Yonehara K, Mizuno N, Inorg. Chem., 2013, 52, 1133.
- [14] Li C, Cao R, Halloran KPO, Ma H, Wu L, Electrochim. Acta 2008, 54, 484.
- [15] Crăciun C, David L, Cozar O, Filip S, Panic I, Analele Univ. Oradea, 2000, 10A, 165.
- [16] Flynn CM, JR, Pope MT, Inorg. Chem. 1971, 10, 2745.
- [17] Himeno S, Takamoto M, Higuchi A, Maekawa M, Inorg. Chim. Acta 2003, 348, 57.
- [18] Hinz M, Näther C, Bensch W, ZAAC, 2013, 2482.
- [19] Wang C, Weng L, Ren Y, Du C, Yue B, Gu M, He H, Z. Anorg. Allg. Chem. 2011, 637, 472.
- [20] Wang X, Zhou B, Zhong C, Ji M, Cryst. Res. Technol. 2006, 41, 874.
- [21] Driss H, Thouvenot R, Debbabi M, Polyhedron 2008, 27, 2059.
- [22] Flynn CM, Pope MT, Inorg. Chem. 1973, 12, 1626.
- [23] Flynn CM, JR., Pope MT, Inorg. Chem. 1971, 10, 2745.
- [24] Sheldrick GM, SHELXS/L-97, Programs for Crystal Structure Determination, University of Göttingen, Göttingen (Germany, 1997).
- [25] Sheldrick GM, Acta Crystallogr. 2008, A64, 112.
- [26] Farrugia LJ, WINGX, A MS-Windows System of Programs for Solving, Refining and Analysing Single Crystal X-ray Diffraction Data for Small Molecules, University of Glasgow, Glasgow (Scotland (UK), 2005).
- [27] Farrugia LJ, J. Appl. Crystallogr. 1999, 32, 837.
- [28] Reyes C, Fernandez J, Freer J, Mondaca MA, Zaror C, Malato S, Mansilla HD, J. Photochem. Photobiol. 2006, A184, 141.
- [29] Ben Said O, Goni-Urriza MS, Elbour M, Dellali M, Aissa P, Duran R, J. Appl. Microbiol. 2008, 104, 987.
- [30] Dunjia W, Zhengdong F, Xianhong W, Wuhan J, University of Technology-Mater. Sci. Ed. 2008, 23(2), 198-203.
- [31] Fumin Z, Maiping G, Hanqing G, Jun W, Front. Chem. Eng. China 2007, 1(3), 296.
- [32] Wang GL, Mi XJ, Li DM, J. Natural Sciences Journal of Harbin Normal University 1997, 13, 75.

- [33] Bannani F, Driss H, Thouvenot R, Debbabi M, *J. Chem. Crystallogr.* 2007, 37, 37.
- [34] Nishikawa K, Kobayashi A, Sasaki YY, *Bull. Chem. Soc. Jpn.* 1975, 48, 889.
- [35] Dmaille PJ, *J. Am. Chem. Soc.* 1984, 106, 7677.
- [36] Kobashi D, Kohara S, Yamakawa J, Kawahara A, *Acta Crystallogr.* 1997, C53, 1523.
- [37] Lu J, Song H, Wang DQ, Niu MJ, *Acta Cryst.* 2010, E66, m599.
- [38] Guillou N, Férey G, *J. Solid State Chem.* 1997, 132, 224.
- [39] Brown ID, Keefe MO, Navrotsky A, Eds. *Structure and Bonding in Crystals*, vol. 2 Academic Press, New York, 1981, 1–30.
- [40] Müller A, Sessoli R, Krickemeyer E, Bögge H, Meyer J, Gatteschi D, Pardi L, Westphal J, Hovemeier K, Rohlfing R, Döring J, Hellweg F, Beugholt C, Schmidtmann M, *Inorg. Chem.*, 1997, 36, 5239.
- [41] Suber L, Bonamico M, Fares V, *Inorg. Chem.*, 1997, 36, 2030.
- [42] Radkov E, Beer RH, *Polyhedron* 1995, 14, 2139.
- [43] Lee KY, Misono M, "Heteropoly compounds" in *Handbook of Heterogeneous Catalysis*, eds; G. Ertl, H. Knozinger, J. Weitkamp, VCH, 1997, 118-131.
- [44] Majoube M, Vergoten G, *J. Mol. Struct.* 1992, 266, 345.
- [45] Son JH, Kwon YU, *Inorg. Chem.* 2004, 43, 1929.
- [46] Franca MCK, Eon JG, Fournier M, Payen E, Mentre O, *Solid State Sci.* 2005, 7, 1533.
- [47] Yerra S, Amanchi SR, Das SK, *J. Mol. Struc.* 2014, 53, 1062.
- [48] Jie L, Yun L, Tao MP, *Chinese J. Struct. Chem.* 2013, 32, 282.
- [49] Dolphin D, Wick AE, *Tabulation of Infrared Spectral Data*; John Wiley & Sons: New York, 1977.
- [50] Tsuboi M, *J. Am. Chem. Soc.* 1957, 79, 1351.
- [51] Khan MI, Cevika S, Hayashi R, *J. Chem. Soc., Dalton Trans.*, 1999, 1651.
- [52] Watras JM, Teplyakov AV, *J. Phys. Chem. B* 2005, 109, 8928.
- [53] Huang W, Todaro L, Yap GPA, Beer R, *J. Am. Chem. Soc.* 2004, 126, 11564.
- [54] Flynn CM, JR, Pope MT, *Inorg. Chem.* 1971, 10, 2524.
- [55] Ociepa BM, Sokołowska ER, D. Michalska, *J. Mol. Struct.* 2012, 49, 1028.
- [56] Armasa SF, Mesa JL, Pizarro JL, Pena A, Chapman JP, Arriortua MI, *Materials Res. Bull.* 2004, 39 1779.
- [57] Ayyappan P, Asnani M, Ramanan A, Piffard Y, *Proc. Indian Acad. Sci. (Chem. Sci.)*, 2003, 115, 33.
- [58] Farahani MM, Shahbazi S, *Inorg. Chem. Commun.* 2012, 15, 297.
- [59] Abia JA, *Bioresources*, 2013, 8, 2924.
- [60] Ueda T, Komatsu M, HojoM, *Inorga. Chim. Acta*, 2003, 344, 77-84.
- [61] Fuchs J, Freiwald J, Hartl W, *Acta Crystallogr.* 1978, B34, 1764.
- [62] Nakamoto K, *Infrared and Raman Spectra of Inorganic and Coordination Compounds*; John Wiley & Sons: New York, 1997.
- [63] Borah G, Bora T, *Indian J. Chem.* 2001, 40A, 216.
- [64] Paul A, Samanta A, *J. Chem. Sci.*, 2006, 118, 335.
- [65] Tauc J, *Mater. Res. Bull.* 1968, 3, 37.
- [66] Kan WQ, Yang J, Liu YY, Ma JF, Kan WQ, Yang J, Liu YY, Ma JF, *Dalton Trans.* 2012, 411, 1062.
- [67] Liu B, Yang J, Yang GC, Ma JF, *Inorg. Chem.* 2013, 52, 84.
- [68] Shu-Ge F, Xiao Z, Xi ZN, Hui YZ, Lei L, Ping HY, *Chinese J. Struct. Chem.*, 2013, 32, 1805.
- [69] Yuana L, Qina C, Wanga X, Lia Y, Wang E, Z. *Naturforsch.* 2008, 63b, 1175.
- [70] Chen D, Shen G, Tang K, Zheng H, Qian Y, *Mater.Res. Bull.* 2003, 38, 1783.
- [71] Hsiao YJ, Chang YS, Chen GJ, Chang YH, *J. Alloy. Compd.* 2009, 471, 259.
- [72] Maalaoui A, Hajsalem A, Ramond NR, Akriche S, *J Clust Sci.* 2014, 25, 1524.
- [73] Kong YM, Pan LN, Peng J, Xue B, Lu J, Dong BX, *Mater. Lett.* 2007, 61, 2393.
- [74] Hasenknopf B, *Front. Biosci.* 2005, 10, 275.
- [75] Yamase T, *J. Mater. Chem.* 2005, 15, 4773.
- [76] Feng YH, Han ZG, Peng J, J. Lu, B. Xue, L. Li, H. Y. Ma, E. B. Wang, *Mater. Lett.* 2006, 60, 1588.
- [77] Atri AM, Cortés PC, Garland MT, Baggio R, Morales K, Soto M, G. Corsini, *J. Chil. Chem. Soc.*, 2011, 56, 786.

- [78] Nagababu P, Naveena J, Latha L, Pallavi P, Harish S, Satyanarayana S, Revue canadienne de microbiologie, 2006, 52(12), 1247-1254.
- [79] Yamin BM, Narimani L, Ibrahim N, ASEM, 2013, 3, 47.
- [80] Yutaka T, Biomed. Res. 2002 , 23, 273.
- [81] Ghorab MM, Ismail ZH, Gawad SMA, Aziem AA, Heteroatom Chem. 2004, 15, 57.,
- [82] Galya T, Sedlarik V, Kuritka I, Sedlarikova J, Saha P, Int. J. Polym. Anal. Character. 2008, 13, 241.
- [83] Sankarraj AV, Electrocatalytic and antibacterial applications of sandwich type polyoxometalates (ProQuest LLC, United Sates, 2008).
- [84] Patrick GL, An introduction to Medicinal Chemistry, Oxford University Press, 1995.

© 2014, by the Authors. The articles published from this journal are distributed to the public under “**Creative Commons Attribution License**” (<http://creativecommons.org/licenses/by/3.0/>). Therefore, upon proper citation of the original work, all the articles can be used without any restriction or can be distributed in any medium in any form.

Publication History

Received	23 rd Oct 2014
Revised	12 th Nov 2014
Accepted	20 th Nov 2014
Online	30 th Nov 2014